Check for updates

A lysine-based 2:1-[α/aza]-pseudopeptide series used as additives in polymeric membranes for CO₂ capture: synthesis, structural studies, and application†

Mohamed I. A. Ibrahim, [ID] *[abc] Xavier Solimando,[a] Loïc Stefan, [ID] [a]
Guillaume Pickaert,[a] Jérôme Babin,[a] Carole Arnal-Herault,[a] Denis Roizard,[d]
Anne Jonquières,[a] Jacques Bodiguel[a] and Marie-Christine Averlant-Petit [ID] *[a]

The current study presents for the first time the synthesis of a new 2:1-[α/aza]-pseudopeptide series possessing charged amino acids (*i.e.*, lysine) and aims at studying the influences of chirality, backbone length, and the nature of the lysine side chains on the conformation of the 2:1-[α/aza]-oligomers in solution using NMR, FTIR spectroscopy and molecular dynamic calculations. The spectroscopic results emphasized the conservation of the β-turn conformation adopted by the trimers regardless of the chirality which demonstrated a noticeable effect on the conformation of homochiral hexamer (**8c**) compared with the hetero-analogue (**8d**). The molecular dynamic calculations predicted that the chirality and the side chain of the lysine residues caused a little distortion from the classical β-turn conformation in the case of short trimer sequences (**7c** and **7d**), while the chirality and the backbone length exerted more distortion on the β-turn adopted by the longer hexamer sequences (**8c** and **8d**). The large disturbance in hexamers from classical β-turn was attributed to increasing the flexibility and the possibility of molecules to adopt a more energetically favorable conformation stabilized by non-classical β-turn intramolecular hydrogen bonds. Thus, alternating D- and L-lysine amino acids in the 2:1-[α/aza]-hexamer (**8d**) decreases the high steric hindrance between the lysine side chains, as in the homo analogue (**8c**), and the distortion is less recognized. Finally, short sequences of aza-pseudopeptides containing lysine residues improve CO₂ separation when used as additives in Pebax® 1074 membranes. The best membrane performances were obtained with a pseudopeptidic dimer as an additive (**6b′**; deprotected lysine side chain), with an increase in both ideal selectivity α_{CO_2/N_2} (from 42.8 to 47.6) and CO₂ permeability (from 132 to 148 Barrer) compared to the virgin Pebax® 1074 membrane.

Introduction

Pseudopeptides are modified peptides containing non-proteinogenic or modified amino acid building blocks or modified peptide bonds.[1] Chemists used the approach of introducing chemical changes in the peptide backbone or side chains in order to improve the physical and chemical properties of the parent peptides, predicting their promising potentials as candidates for medicinal, environmental and industrial applications.[2–6] Among the modifications in the peptide backbone are those occurring on the amide bond leaving the side chains without any changes.[7] Peptide backbones can be modified in various ways either by extending the peptide chain by one more atom (s) or by changing at least one peptide bond with an isosteric or isoelectronic surrogate, depsipeptide, keto-methylene isoester,[8] azapeptide,[8,9] retro-inverso,[10,11] aminoxy acid,[12,13] hydrazino acid,[14,15] or β-amino acid.[16] Interestingly, Gellmann investigated the ability of some pseudopeptides to self-organize in solution to give stable, reproducible secondary structures that mimic protein secondary structures such as helices, sheets or turns, also known as "Foldamers". The term "Foldamer" as proposed by Gellmann consists of the two words "folding + unnatural oligomer or polymer" which refer to unnatural polymers or oligomers that have a strong tendency to self-organize into a predictable well defined compact structure in solution.[17]

[a]Université de Lorraine, CNRS, LCPM, F-54000 Nancy, France. E-mail: ibrahimmmohamed2030@gmail.com

[b]National Institute of Oceanography and Fisheries, NIOF, Egypt. E-mail: m.ibrahim@niof.sci.eg

[c]Hiroshima Synchrotron Radiation Center, Hiroshima University, 2-313 Kagamiyama, Higashi-Hiroshima, Hiroshima 739-0046, Japan. E-mail: ibra2020@hiroshima-u.ac.jp

*[d]Université de Lorraine, CNRS, LRGP, F-54000 Nancy, France*

For several decades, our laboratory has demonstrated the design, synthesis and conformational study of pseudopeptide oligomers.[18–20] Specifically, we have been focused on pseudo-peptidic bis-nitrogen compounds such as hydrazinopeptides,[21–23] N-aminopeptides.[24–26] More recently, we have extended the interests on the synthesis and conformational study of azapeptides[20,27–31] in which the α-carbon(s) of one or more of the amino acid residues is/are replaced with one or more nitrogen atom(s) in the peptide sequence.[9,32–35] Azapeptides have been studied since the early sixties and actively developed by Gante[9] and by Dutta and Morley.[36] Synthesis of azapeptides has been particularly investigated by Gante[9,33,34] and our group[20,27,29–31,37] in liquid-phase peptide synthesis, and by Gray *et al.*[38] in solid-phase. Interestingly, several studies demonstrate that the insertion of an aza-residue into a peptide backbone has intense effects not only on the geometrical structure, but also on its physical and chemical properties. Among the impact of such chemical modification, we can mention that: (i) the CO–N amide bonds are elongated by 0.03 Å (ref. 39) while the N–N$^\alpha$ and N$^\alpha$–CO bonds are shortened by 0.06 Å compared to N–C$^\alpha$ and C$^\alpha$–CO in the natural peptide; (ii) the N–N$^\alpha$–CO angle is larger by about 4–5° than the N–C$^\alpha$–CO bond angle; (iii) the substituted nitrogen atom N$^\alpha$ adopts chiral property with a pyramidal nature of sp^3 type;[18,39] (iv) the flexi-bility is reduced in the formed azapeptides compared with the parent one due to the replacement of the rotatable C$^\alpha$–C(O) bond by a more rigid urea N$^\alpha$–C(O) structure; and (v) an elec-tronic repulsion of the lone pairs of the two adjacent nitrogens restricts motion of the dihedral angle (ϕ).[40,41] Thus, based on these data, the conformational restrictions in the azapeptides which bend the peptide backbone at the aza-amino acid residue away from a linear geometry, could be predicted.[42] Several spectroscopic,[21,43–46] crystallographic,[18,21,37,47,48] and computational[41,43,49–52] studies demonstrate the ability of aza-peptides to induce β-turn conformations of type I, type II, and type VI when aza-residue occupying the position ($i + 1$) or ($i + 2$) in the peptide sequence, stabilized by intramolecular hydrogen bonds.[18,19,21,43,46,49,52]

Previous studies[30,31] have proved, using FTIR, NMR spec-troscopy techniques as well as molecular dynamic calculations, the propensity of the azapeptides (**7a**, **7b**, **8a**, and **8b**, Scheme 1) to adopt β-turn conformations stabilized by intramolecular hydrogen bonds in both solution and solid states. However, there are not much reported studies concerning the effect of introducing charged amino acid in azapeptides sequences on their conformations. Consequently, we decided to focus our attention to the synthesis and studies of new 2:1-[α/aza]-oligomers containing charged amino acid moieties such as lysine. Indeed, we suggested that the incorporation of basic amino acid(s) (lysine) with supplementary nitrogen atom N$^\varepsilon$H in its/their side chain(s) may: (i) produce oligomers with good selectivity in gases separation, especially (N$_2$/CO$_2$) by membrane technology, and (ii) increase the hydrophilicity of the final oligomers which may support the formation of hydrogels with promising potential applications.

In this context, the current work focus on the synthesis of new series of 2:1-[α/aza]-oligomers possessing lysine residues in
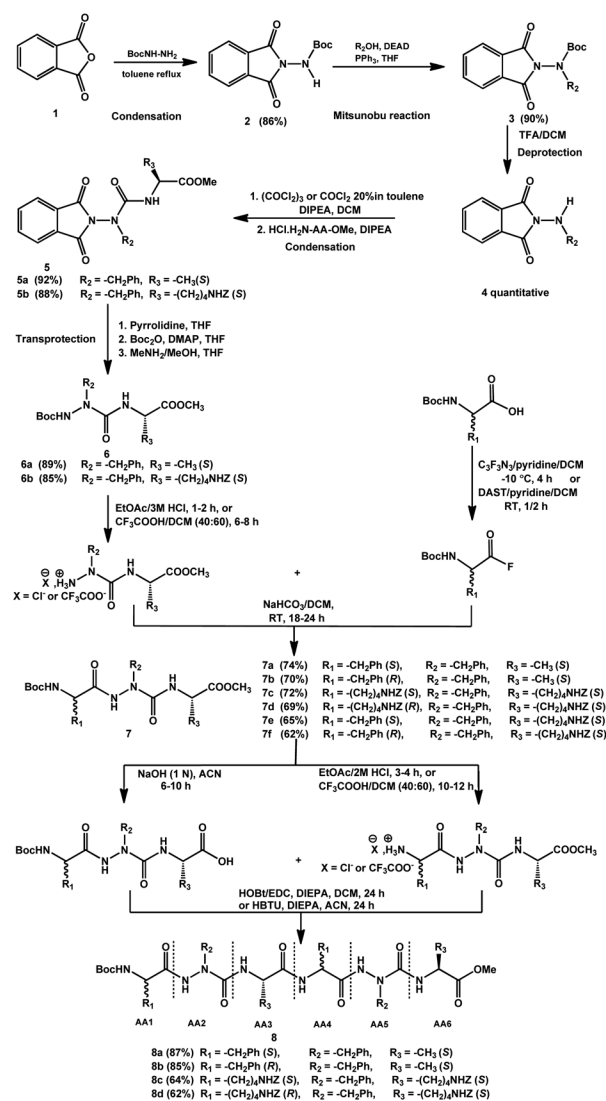
Scheme 1 General stepwise strategy for the synthesis of new series of 2:1-[α/aza]-oligomers based lysine amino acid residue.[30,31]

solution state. Then, the conformational studies of some synthesized oligomers (**7c**, **7d**, **8c** and **8d**, Scheme 1) were elucidated in solution state using spectroscopic techniques (NMR and FTIR) and molecular dynamic calculations (Amber 12). In addition, the work extended to test a selection of these azapeptide oligomers as new pseudopeptide-based additives for gas separation membranes for CO$_2$ capture. The study focused on the influence of the azapeptide oligomer length and of the nature of the side group of the amino acids (with or without protected or non-protected lysine residues) on the gas perme-ation properties of Pebax® 1074 membranes containing the new bio-inspired additives.

Experimental section

General

Unless otherwise stated, all chemicals and reagents were purchased from commercial suppliers (Sigma-Aldrich, Fluka,

Merck or Alfa-Aesar). Dry CH_2Cl_2 was obtained by distillation over P_2O_5 under an argon atmosphere, MeOH was purchased in anhydrous form, and other reagent-grade solvents were used without further purification as received. Reactions were monitored by thin-layer chromatography (TLC) using aluminum-backed silica gel plates. TLC spots were viewed under UV light or/and by heating the plate after treatment with a staining solution of phosphomolybdic acid. Flash chromatography was carried out on silica gel 60 (0.04–0.063 μm Mesh ASTM). All yields were calculated from pure isolated products. Electron spray ionization mass spectra (ESI-MS) were recorded with a Bruker MicroTof-Q HR spectrometer. All melting points (mp) were uncorrected.

NMR spectroscopy

1D (^{1}H and ^{13}C) and 2D (ROESY) NMR spectra were recorded using a Brucker Advance NMR spectrophotometer (300 MHz) in $CDCl_3$, CD_3CN and DMSO-d_6 as solvents at room temperature with chemical shifts of 7.26, 1.94 and 2.50 ppm, respectively. The chemical shifts were reported in ppm (δ) relative to tetramethylsilane (TMS) served as an internal standard ($\delta = 0$ ppm) for ^{1}H NMR, while $CDCl_3$ ($\delta = 77.16$ ppm), CD_3CN ($\delta = 1.32$ & 118.26 ppm) and DMSO-d_6 ($\delta = 39.5$ ppm), were used as internal standards for ^{13}C NMR. Multiplicities are reported as follows: s = singlet, d = doublet, q = quartet, m = multiplet, br = broad, arom = aromatic.

Fourier transform infrared spectroscopy

FTIR spectra for all products in $CDCl_3$ were recorded with Bruker Tensor 27 over 128 scans and referenced to the residual solvent resonances. In addition, attenuated total reflectance (ATR-FTIR) measurements have been performed on solids for some products. All the spectra were recorded on Bruker Tensor 27 spectrometer equipped with a trough plate comprising of a germanium single crystal where the samples were loaded over it. Spectra were acquired in the 4000–400 cm^{-1} range with a resolution of 4.0 cm^{-1} over 128 scans, taken into consideration the background subtraction from each spectrum to correct for atmospheric interference.

Molecular dynamic calculations (AMBER 12)

Calculations on molecules (**7c**, **7d**, **8c**, and **8d**) were carried out according to the protocol: 0.5 μs with 2 fs steps molecular dynamics simulations were calculated in explicit solvent (chloroform; $CHCl_3$ box) without any ROE constraints under constant pressure periodic boundary conditions, pressure relaxation time of 0.5 μs, and constant temperature 300 K, using the package of molecular dynamics simulation programs AMBER 12. The starting molecules were constructed using MarvinSketch (ChemAxon), Antechamber and Xleap from AMBER program suite. Molecular simulation was done with Sander program with general AMBER force field (GAFF) and included amino acid parameters (ff99SB). Ptraj was employed for the analysis of 25 000 structures.[53,54]

Synthesis of *N-tert*-butyloxycarbonylaminophtalimide (2)

Phthalic anhydride (1.0 equiv.) and tertbutylcarbazate (1.0 equiv.) were dissolved in toluene in a monocol with a Dean–Stark. The suspension is refluxed for 12 h. The mixture was cooled and the *N-tert*-butyloxycarbonylaminophtalimide **2** precipitated. The solid was filtered off and recrystallized with EtOAc.

Synthesis of *N*-benzyl-*N-tert*-butyloxycarbonylaminophtalimide (3)

To a solution of *N-tert*-butyloxycarbonylaminophtalimide **2** (1.0 equiv.), PPh_3 (1.5 equiv.) and benzyl alcohol (3.0 equiv.) in dry THF, DEAD (1.5 equiv.) was added in one portion under N_2 and stirring at 0–5 °C. The resulting solution was stirred overnight (monitored by TLC until completion) and concentrated under vacuum. The residue was triturated in EtOAc, placed in a refrigerator and most of the triphenylphosphine oxide was precipitated which then removed by filtration. The filtrate was evaporated, and the residue was purified by column chromatography on silica gel.

Synthesis of *N*-alkylaminophtalimide (4)

To a solution of *N*-alkyl-*N-tert*-butyloxycarbonylaminophtalimide **3** (1.0 equiv.) in CH_2Cl_2, trifluoroacetic acid (10.0 equiv., 8.0% in CH_2Cl_2) was added at 0 °C. The mixture was stirred overnight (monitored by TLC). The solution was concentrated under vacuum, and then the residue was dissolved in CH_2Cl_2, neutralized with a saturated solution of $NaHCO_3$ (pH = 7) and extracted three times with CH_2Cl_2. The combined organic layers were dried over $MgSO_4$ and evaporated under vacuum giving a yellow solid which was immediately used without further purification.

Synthesis of Pht-azaPhe-Ala-OMe (5a)

To a mixture of *N*-alkyl-aminophtalimide (**4**) (1.0 equiv.) and DIPEA (2.2 equiv.) in dry CH_2Cl_2, phosgene 20% in toluene (1.5 equiv.) was added. After 15 min stirring, the toluene solvent and excess of phosgene gas were removed by rotary evaporator under ventilated hood. The white acid chloride residue was re-dissolved in dry CH_2Cl_2, then solution of alanine methyl ester hydrochloride (1.0 equiv.) and DIPEA (1.5 equiv.) in dry CH_2Cl_2 was added in one portion. The reaction mixture was stirred for 1 h at RT. The solvent was evaporated to dryness, diluted with CH_2Cl_2, washed with aqueous HCl (1 N), aqueous $NaHCO_3$ (1 N) and brine, dried over $MgSO_4$ and evaporated. Compound **5a** was obtained in pure form after precipitation in cold diethyl ether.

Synthesis of Pht-azaPhe-Lys(z)-OMe (5b)

To a mixture of *N*-alkyl-aminophtalimide (**4**) (1.0 equiv.) and DIPEA (2.2 equiv.) in dry CH_2Cl_2, phosgene 20% in toluene (1.5 equiv.) was added. After 15 min stirring, the toluene solvent and excess of phosgene gas were removed by rotary evaporator under ventilated hood. The white acid chloride residue was further re-dissolved in dry CH_2Cl_2, then solution of lysine(Z) methyl ester hydrochloride (1.0 equiv.) and DIPEA (1.5 equiv.) in dry CH_2Cl_2 was added in one portion. The reaction mixture was

stirred for 1 h at RT. The solvent was evaporated to dryness, diluted with CH_2Cl_2, washed with aqueous HCl (1 N), aqueous $NaHCO_3$ (1 N) and brine, dried over $MgSO_4$ and evaporated. Compound **5b** was obtained in pure form after precipitation in cold EtOAc.

Synthesis of Boc-azaPhe-Ala-OMe (6a)

To a solution of Phth-azaPhe-Ala-OCH$_3$ (**5a**) (1.0 equiv.) in THF, pyrrolidine (3.0 equiv.) was added at RT. The mixture was stirred at RT until completion (4 h, monitored by TLC). The solvent and the excess of amine were removed under vacuum giving foam residue. The obtained residue was dissolved in THF, then Boc_2O (1.5 equiv.) and a catalytic amount of DMAP (0.15 equiv.) were added. The mixture was stirred at RT until completion (12 h, monitored by TLC). The solvent was removed under vacuum, the residue was dissolved in THF and a freshly prepared solution of methylamine (1.5 equiv., 2 M in MeOH) was added at RT. The mixture was stirred at RT until completion (12 h, monitored by TLC), the solvent and the excess of amine were removed under vacuum and the residue was purified by column chromatography on silica gel.

Synthesis of Boc-azaPhe-Lys(z)-OMe (6b)

To a solution of Phth-azaPhe-Lys(z)-OCH$_3$ (**5b**) (1.0 equiv.) in THF, pyrrolidine (3.0 equiv.) was added at RT. The mixture was stirred at RT until completion (5 h, monitored by TLC). The solvent and the excess of amine were removed under vacuum giving foam residue. The obtained residue was dissolved in THF, then Boc_2O (1.5 equiv.) and a catalytic amount of DMAP (0.15 equiv.) were added. The mixture was stirred at RT until completion (12 h, monitored by TLC). The solvent was removed under vacuum, the residue was re-dissolved in THF and a freshly prepared solution of methylamine (1.5 equiv., 2 M in MeOH) was added at RT. After a night and by TLC monitoring, the solvent and the excess of amine were removed under vacuum and the residue was purified by column chromatography on silica gel. The volume of the THF during the second step (addition of Boc_2O) is twice the volume used for the first and third steps (pyrrolidine or methyl amine) to inhibit the reactivity of the N^εH of lysine in concentrated condition.

General protocol for the synthesis of 2:1-[α/aza]-trimers

Boc deprotection. To a stirred solution of Boc protected compound (**6**) (1.0 equiv.) in CH_2Cl_2, ethyl acetate (3.0 M HCl) was added at 0 °C. The resulting solution was stirred until completion (1–2 h, monitored by TLC) and concentrated under vacuum. The excess hydrochloride acid was co-evaporated with CH_2Cl_2 (4 times). The residue was used in coupling reaction without further purification.

Acid fluoride preparation. To a stirred solution of Boc-D- or L-AA-OH (1.5 equiv., AA = Phe, Lys(z), D-Phe, or D-Lys(z)) in dry CH_2Cl_2 and pyridine (1.5 equiv.) kept under a N_2 atmosphere, cyanuric fluoride (3.0 equiv.) was added dropwise at −20 °C. The solution was stirred at −10 °C during 4 h and a precipitate or emulsion formed, and its amount gradually increased. Then, crushed ice was added along with an additional cold CH_2Cl_2.

The organic layer was separated, and the aqueous layer extracted with cold CH_2Cl_2. The combined organic layers were washed with ice-cold water and dried over $MgSO_4$, and the solvent was removed with a rotary evaporator at room temperature to yield the acyl fluoride product which was directly used in the coupling reaction.

Coupling reaction. Boc-D- or L-AA-F (1.5 equiv., AA = Phe, or Lys(z)) in CH_2Cl_2 was added dropwise to a stirred solution of HCl, H-azaPhe-AA-OMe (1.0 equiv., AA = Ala, or Lys(z)) in CH_2Cl_2 and $NaHCO_3$ (2.0 equiv.), pH = 7–8. The mixture was stirred at RT overnight monitoring by TLC. Then, the organic layer (CH_2Cl_2) was washed twice with HCl (1 N), $NaHCO_3$ (1 N) and saturated NaCl, and then was dried over $MgSO_4$ and the solvent was removed under vacuum and the residue was purified by column chromatography on silica gel.

General protocol for the synthesis of 2:1-[α/aza]-oligomer

Homo and heterochiral 2:1-[α/aza]-hexamers (**8**) were obtained by classical peptidic coupling based on the monomeric building blocks of 2:1-[α/aza]-trimers (**7**).

Boc deprotection. To a stirred solution of Boc protected compound (**7**, 1.0 equiv.) in CH_2Cl_2, ethyl acetate (2 M HCl) was added at 0 °C. The resulting solution was stirred until completion monitored by TLC (2–4 h) and concentrated under vacuum. The excess of hydrochloric acid was co-evaporated with CH_2Cl_2 (4 times). The residue was used in coupling reaction without further purification.

Methyl ester deprotection. To a stirred solution of methyl ester protected compound (**7**, 1.0 equiv.) in CH_3CN, an aqueous solution of NaOH 1 N (2.0 equiv.) was added at 0 °C. The resulting solution was stirred until completion monitored by TLC (4–10 h), then aqueous HCl (2 N) was added under vigorously stirring (pH = 2). The aqueous layer was extracted twice with CH_2Cl_2, then the combined organic layers were dried over $MgSO_4$ and evaporated. The residue was used in coupling reaction without further purification.

Coupling reaction. To a stirred solution of the Boc-deprotected trimer (amine partner, 1.0 equiv.) in CH_2Cl_2 were successively added at RT; DIPEA (2.2 equiv.), deprotected methyl ester trimer (acid partner, 1.1 equiv.) and HOBt (1.2 equiv.). After a night to 24 h, the mixture was diluted with aqueous HCl (1 N) under vigorously stirring (pH = 2). The organic layer was washed with water, aqueous $NaHCO_3$ (0.5 N), brine, dried over $MgSO_4$ and evaporated. The residue was purified by column chromatography on silica gel.

It should be mentioned that the better yields of hexamers containing lysine residues (**8c** and **8d**) were obtained upon carrying the coupling reaction in CH_3CN with HBTU/DIPEA.

Synthesis of 6b′, 7c′ and 8c′ molecules by deprotection of Z-group from the corresponding protected analogues

To a stirred solution of an appropriate protected side chain(s) azapeptide (200 mg) in methanol (5.0 mL), 10% Pd/C (20 mg per each Z-group) was added. The resulting reaction mixture was stirred under stream of H_2 gas at room temperature. After completion of the hydrogenolysis (4–12 h), the mixture was

Paper

filtered through a Celite bed and washed with methanol. The combined filtrates were evaporated and then the residue was dried well under vacuum before verification by ^{1}H NMR in DMSO-d_6. The deprotection was considered to be successfully achieved if the signals belong to the CH$_2$ and the aromatic protons of Z-group have been disappeared in the ^{1}H NMR spectrum.

Membrane preparation. For membrane casting, the Pebax®1074 polymer and pseudopeptide additives were dissolved in *n*-butanol during 2 h at 80 °C to obtain a total concentration of 2.5 w/v%. Different series of membranes were prepared using the same weight percentage (4.0 wt%) for each pseudopeptide in the different membranes. After filtering on glass fibers, the solutions were cast on a PTFE mold. After butanol evaporation in a thermal oven at 40 °C, the membranes were easily taken off the mold and were then dried under vacuum at 60 °C for 12 h. Their thicknesses were measured with an Elcometer™ micrometer after calibration in the thickness range of interest (measurement error: ±1 μm). The average thickness for the different membranes was *ca.* 80 μm with a maximum thickness difference between two membrane points of 5 μm.

Gas permeation experiments. The gas permeation properties were determined by the "time-lag" method using an experimental procedure described in our former work on other bio-based pseudopeptide for CO_2 capture membranes.[55] The gas permeation properties were determined for CO_2 and N_2 pure gases (high purity gases purchased from Messer Company) at 35 °C and 2 bar. The gas permeation experiments were repeated five times for each membrane and each tested gas to assess the reproducibility from the corresponding experimental errors.

The gas permeability was calculated from the steady-state membrane flux J_{st} estimated from the steady-state slope of the gas permeation curve (describing the pressure increase with time at the membrane downstream side) and the membrane thickness l according to eqn (1). In this equation, the downstream side pressure was neglected as usual for "time-lag" experiments because it was much lower than the upstream side pressure of 2 bar:

$$P = \frac{J_{st} \times l}{\Delta p} = \frac{J_{st} \times l}{p_{upstream}} \quad (1)$$

The membrane ideal selectivity was estimated as the ratio of the permeability for pure CO_2 and N_2 according to eqn (2):

$$\alpha_{CO_2/N_2} = \frac{P_{CO_2}}{P_{N_2}} \quad (2)$$

The gas diffusion coefficient D was calculated from the "time-lag" q given by the intercept of the steady-state asymptote of the gas permeation curve on the time axis by eqn (3).

$$D = \frac{l^2}{6\theta} \quad (3)$$

Gas permeability is the product of gas diffusion and sorption coefficients according to the solution–diffusion model

expressed by eqn (4), describing gas permeation in the dense (non-porous) membranes used in this work:[56]

$$P = D \times S \quad (4)$$

Consequently, the gas sorption coefficient (S) was then calculated as the ratio of the permeability (P) to the diffusion coefficient (D).

Results and discussion

Azapeptides of two to six uncharged amino acids residues were successfully synthesized in our previous studies in excellent yields and the coupling reactions were controlled mainly by the chemistry protocol including the efficiency of the coupling reagents.[30,31] In the current study, the experimental conditions might not the only factors controlling the coupling reactions, while the kinetics and thermodynamic parameters seem to influence the coupling yields which were not studied here (Table 1). The side chain of lysine residues is highly flexible and can form intra- and/or intermolecular hydrogen bonds in solution with either the main backbone or neighboring molecules, affecting the coupling yields, particularly for longer azapeptides (**8a** & **8b** *versus* **8c** & **8d**; Table 1).

The general stepwise strategy used to design a new series of 2:1-[α/aza]-oligomers is mainly based on the protocol discussed and reported in previous studies, depicted Scheme 1.[30,31] Various homo and hetero 2:1-[α/aza]-oligomers *i.e.*, six trimers (**7a–7f**) and four hexamers (**8a–8d**) were synthesized in good yields after purification by silica column chromatography as summarized in Table 1. Detailed characterization data are provided as ESI.†

NMR and FTIR spectroscopic studies of 2:1-[α/aza]-trimers

^{1}H NMR studies of compounds (**7c**) and (**7d**) were carried out at dilute concentration in CDCl$_3$ (3.0 mmol L^{-1}, 300 K) to avoid intermolecular interactions. The spectra showed well resolved signals and the CH$_2$ protons of the azaPhe moiety are non-equivalent magnetically (ESI, Fig. S1 and S2†). In addition, 2D NMR (ROESY) experiments for compound (**7c**) revealed the presence of a moderate correlation between the protons of C^{α}H (Lys1) and the NH (azaPhe), as well as a weak correlation between the protons of NH (azaPhe) and NH (Lys2) (ESI, Fig. S3†). The same ROE correlations were observed for compound (**7d**) (ESI, Fig. S4†) with also moderate and weak correlations between C^{α}H (D-Lys1) and the NH (azaPhe) protons, and between the NH (azaPhe) and NH (Lys2) protons, respectively. These results indicate that the molecules (**7c**) and (**7d**) may induce βII- and βII′-turn conformations in solution, respectively, Fig. 1.[30,49,57]

The βII-turns which are often stabilized *via* intramolecular hydrogen bonds, were investigated by studying the effect of solvent composition by NMR technique. The method measures the sensitivity of the NH protons through their chemical shift variations as a function of the [CDCl$_3$/DMSO-d_6] ratio.[44] The results (Fig. 2a and b) demonstrated that most of the NH protons of (**7c**) and (**7d**) were sensitive to the addition of DMSO-

Table 1 Yields (%) and physical characteristics of the synthesized 2:1-[α/aza]-oligomers

| ID	Compound	Yield (%)	Physical characteristics data
2	*N-tert-*Butyloxycarbonylaminophtalimide	86	White crystal after recrystallization by ethyl acetate. HRMS (ESI) for [$C_{13}H_{14}N_2O_4$]: calculated [M + H]$^+$ (*m/z*) 263.0954; found, 263.1034
3	*N*-Benzyl-*N-tert*-butyloxy-carbonylaminophtalimide	90	White solid after flash chromatography (0.04–0.063 μm) using eluent (15% ethyl acetate : 85% petroleum ether); mp 107–109 °C. HRMS (ESI) for [$C_{20}H_{20}N_2O_4$]: calculated [M + Na]$^+$ (*m/z*) 375.1321; found, 375.1314
4	*N*-Alkylaminophtalimide	∼100	Quantitative yellow powder without purification; mp 109–110 °C; HRMS (ESI) for [$C_{15}H_{12}N_2O_2$]: calculated [M + H]$^+$ (*m/z*) 253.0977; found, 253.0963
5a	Pht-azaPhe-Ala-OMe	92	Pure white powder after trituration with cold diethyl ether; mp 158–161 °C. HRMS (ESI) for [$C_{20}H_{19}N_3O_5$]: calculated [M + Na + MeOH]$^+$ (*m/z*) 436.1479; found, 436.1457
5b	Pht-azaPhe-Lys(z)-OMe	88	Pure white solid after precipitation with cold ethyl acetate; mp 134–135 °C. HRMS (ESI) for [$C_{31}H_{32}N_4O_7$]: calculated [M + Na]$^+$ (*m/z*) 595.2169; found, 595.2170; calculated [M + K]$^+$ (*m/z*) 611.3254; found, 611.1909
6a	Boc-azaPhe-Ala-OMe	89	White solid after flash chromatography using 30% ethyl acetate : 70% petroleum ether; mp 90–91 °C. HRMS (ESI) for [$C_{17}H_{25}N_3O_5$]: calculated [M + H]$^+$ (*m/z*) 352.1872; found, 352.1878
6b	Boc-azaPhe-Lys(z)-OMe	85	An oily sticky product after flash chromatography using 45% ethyl acetate : 55% petroleum ether. HRMS (ESI) for [$C_{28}H_{38}N_4O_7$]: calculated [M + Na]$^+$ (*m/z*) 565.2638; found, 565.2643; calculated [M + K]$^+$ (*m/z*) 581.3723; found, 581.2377
7a	Boc-Phe-azaPhe-Ala-OMe	74	White solid after flash chromatography using 50% ethyl acetate : 50% petroleum ether; mp 149–150 °C. HRMS (ESI) for [$C_{26}H_{34}N_4O_6$]: calculated [M + Na]$^+$ (*m/z*) 521.2376; found, 521.2344
7b	Boc-D-Phe-azaPhe-Ala-OMe	70	White solid after flash chromatography using 50% ethyl acetate : 50% petroleum ether; mp 72–73 °C. HRMS (ESI) for [$C_{26}H_{34}N_4O_6$]: calculated [M + Na]$^+$ (*m/z*) 521.2376; found, 521.2389
7c	Boc-Lys(z)-azaPhe-Lys(z)-OMe	72	White foam after flash chromatography using 60% dichloromethane : 38.5% ethyl acetate : 1.5% methanol. HRMS (ESI) for [$C_{42}H_{56}N_6O_{10}$]: calculated [M + Na]$^+$ (*m/z*) 827; 3956 found, 827.3978; calculated [M + K]$^+$ (*m/z*) 843.3695 found, 843.3715
7d	Boc-D-Lys(z)-azaPhe-Lys(z)-OMe	69	White foam after flash chromatography using 60% dichloromethane : 38.5% ethyl acetate : 1.5% methanol. HRMS (ESI) for [$C_{42}H_{56}N_6O_{10}$]: calculated [M + Na]$^+$ (*m/z*) 827.3956 found, 827.3986; calculated [M + K]$^+$ (*m/z*) 843.3695 found, 843.3714
7e	Boc-Phe-azaPhe-Lys(z)-OMe	65	White foam after flash chromatography using 70% dichloromethane : 29% ethyl acetate : 1.0% methanol. HRMS (ESI) for [$C_{37}H_{47}N_5O_8$]: calculated [M + Na]$^+$ (*m/z*) 712.3322 found, 712.3339; calculated [M + K]$^+$ (*m/z*) 728.3062 found, 728.3042
7f	Boc-D-Phe-azaPhe-Lys(z)-OMe	62	White foam after flash chromatography using 70% dichloromethane : 29% ethyl acetate : 1.0% methanol. HRMS (ESI) for [$C_{37}H_{47}N_5O_8$]: calculated [M + Na]$^+$ (*m/z*) 712.3322 found, 712.3327; calculated [M + K]$^+$ (*m/z*) 728.3062 found, 728.3028
8a	Boc-(Phe-azaPhe-Ala)$_2$-OMe	87	White solid after flash chromatography using 60% ethyl acetate : 40% petroleum ether; mp 132–133 °C. HRMS (ESI) for [$C_{46}H_{56}N_8O_9$]: calculated [M + Na]$^+$ (*m/z*) 887.4062 found, 887.4068
8b	Boc-(D-Phe-azaPhe-Ala)$_2$-OMe	85	White solid after flash chromatography using 60% ethyl acetate : 40% petroleum ether; mp 172–173 °C. HRMS (ESI) for [$C_{46}H_{56}N_8O_9$]: calculated [M + Na]$^+$ (*m/z*) 887.4062 found, 887.4066
8c	Boc-(Lys(z)-azaPhe-Lys(z))$_2$-OMe	64	White foam after flash chromatography using 50% dichloromethane : 48% ethyl acetate: 2% methanol. HRMS (ESI) for [$C_{78}H_{100}N_{12}O_{17}$]: calculated [M + Na]$^+$ (*m/z*) 1499.7227, found, 1499.7181; calculated [M^{2+}+Na] (*m/z*) 761.3615, found 761.3664
8d	Boc-(D-Lys(z)-azaPhe-Lys(z))$_2$-OMe	62	White foam after flash chromatography using 50% dichloromethane : 48% ethyl acetate : 2% methanol. HRMS (ESI) for [$C_{78}H_{100}N_{12}O_{17}$]: calculated [M + Na]$^+$ (*m/z*) 1499.7227, found, 1499.7153; calculated [M^{2+}+Na] (*m/z*) 761.3615, found 761.3592
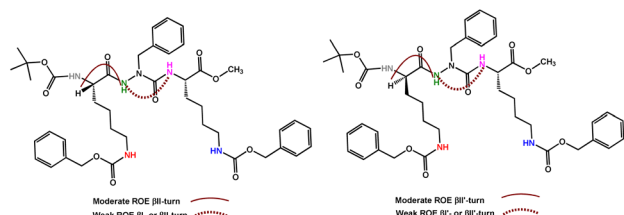
Fig. 1 ROE correlations of βII- and βII′-turn conformations in **7c** (left) and **7d** (right), respectively; (300 MHz, 3.0 mmol L^{-1}, CDCl$_3$, 300 K).
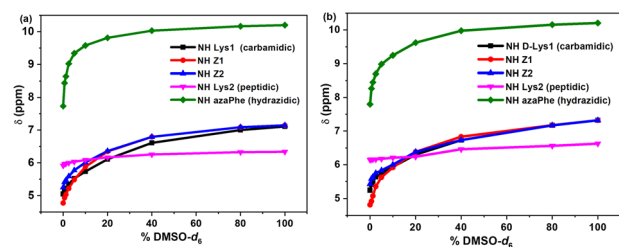

Fig. 2 Chemical shift-variations (δ) of HN protons for: (a) **7c**, and (b) **7d** as a function of % [CDCl$_3$/DMSO-d_6] mixtures.

d_6, while the NH (Lys2) are weakly perturbed. These results suggest that only the NH (Lys2) might be involved in intramolecular hydrogen bonds, in contrast to all the other free NH protons (*i.e.*, NH (Lys1 or D-Lys1), NH (azaPhe), and N$^\varepsilon$H of lysine side chains) for which high chemical shifts variations are observed at high % DMSO-d_6 (ESI, Fig. S5†).

The existence of certain conformation and intramolecular hydrogen bonds within the compounds (**7c**) and (**7d**) were further identified using IR in dilute condition (3.0 mmol L^{-1}, CDCl$_3$), focusing on the two characteristic NH and CO stretching regions. For compound (**7c**), the NH region reveals the presence of free NH band around 3449 cm^{-1} belongs to the free amide proton (Lys1), N$^\varepsilon$H (Lys1 + Lys2) and hydrazino NH

Fig. 3 FTIR spectra belong to the NH stretching region (up spectra), and CO stretching region (bottom spectra) for: (a and c) **7c**, and (b and d) **7d** (3.0 mmol L^{-1}, CDCl$_3$).

(azaPhe), in addition to a very broad band with a maximum at 3378 cm^{-1} related to the bound Lys2 amide NH proton (Fig. 3a). The NH stretching region of compound (**7d**) shows the presence of two characteristic bands centered at 3449 cm^{-1} corresponding to the free NH (Lys1), N$^\varepsilon$H (D-Lys1 + Lys2) and NH (azaPhe), and at 3375 cm^{-1} (very broad), assigned to the bound NH (Lys2). Moreover, in Fig. 3b, there is an additional band at 3302 cm^{-1} which supposed that N$^\varepsilon$H proton of the lysine is involved in a weak an intramolecular hydrogen bond. These results for both compounds are agreed with the NMR solvent composition study.

Regarding the CO vibration region, the two spectra are very similar with broadening and overlapping of the CO groups which was solved by the help of the 2nd derivative deconvolution method (Fig. 3c, d). The assignment of the CO groups of (**7c**) and (**7d**) were based on their small precursors and previously studied oligomers belong to the same series.[30,31] Subsequently, seven bands could be assigned (ESI, Table S1†), particularly the band at 1652 cm^{-1} which was assigned to the CO of the Boc group involved in a hydrogen bond. Accordingly, the NH (Lys2) in both compounds (**7c**) and (**7d**) was assumed to be involved in intramolecular hydrogen bonds with the CO (Boc) which stabilizes the β-turn conformation *via* a pseudocycle of 10 atoms (Fig. 1), while the other CO groups are in free states in dilute solution, as noticed from their higher frequencies.[30,31]

Molecular dynamic calculations of 2:1-[α/aza]-trimers

In order to investigate the major conformation(s), as well as the possible intramolecular hydrogen bonds in the 2:1-[α/aza]-oligomers (trimers and hexamers), molecular dynamic calculations for the four molecules (**7c**, **7d**, **8c** and **8d**) were carried out according to the protocol described in experimental section using AMBER software package. Each trajectory carry 25 000 structures for each molecule. AMBER module Ptraj was employed for their analysis in order to assess the possible existence of hydrogen bond and the average values of the torsion angles. It has been reported that the secondary structure of azapeptides is based on the structural backbone elements which composed of the hydrazine and an urea constituent, in which the two parts are described by the torsion angles ϕ and ψ, respectively (ESI, Fig. S6†).[49]

The statistical analysis of the dihedral angles for each simulated 25 000 structures suggests that Boc-Lys(z)-azaPhe-Lys(z)-OMe (**7c**) adopts distorted βIV-turn conformation between the three residues, however Boc-D-Lys(z)-azaPhe-Lys(z)-OMe (**7d**) deviated largely from the βI′-turn conformation as noticed specifically from the values $\phi_1 = 128.4°$ and $\psi_1 = -64.94°$ (ESI, Table S2†). The deviation in the dihedral angles [(**7c**) > (**7d**)] may be explained, first by the flexibility of the compounds' structures which mainly associated with the presence of additional interactions, causing disturbance in the torsional angles. These results are consistent with the FTIR spectra which showed only one broad band for (**7c**), while two bands for (**7d**), predicting the high torsion angles' distortion in (**7d**) compared to (**7c**) by the additional intramolecular hydrogen bonds.
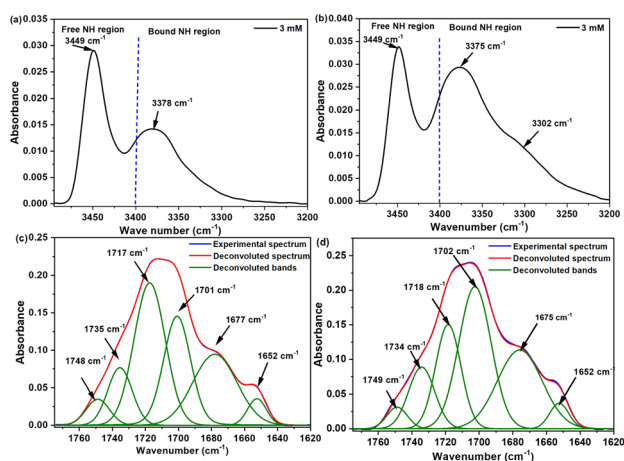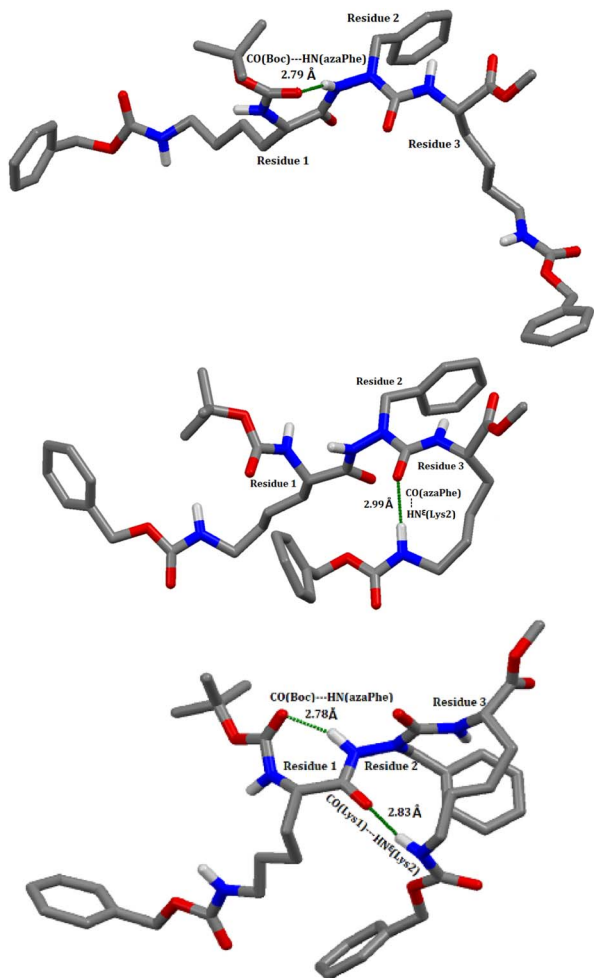
Fig. 4 Selected frames for (**7c**) obtained by molecular dynamic simulations, illustrating different intramolecular hydrogen bonds (green dots); type i (upper), type ii (middle), and types i & ii (below). The H atoms, except those of the NH groups, have been omitted for clarity.
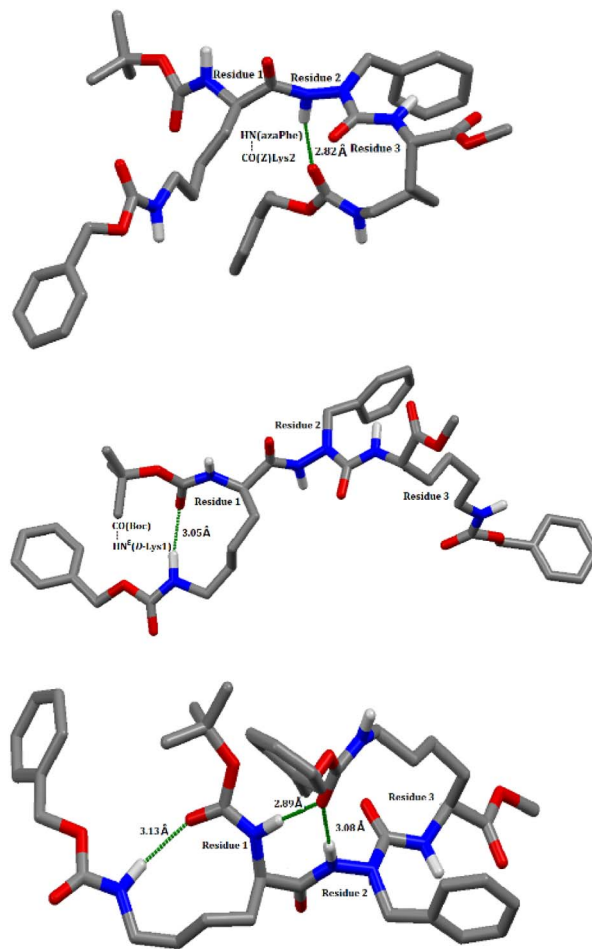

Fig. 5 Selected frames for (**8c**) obtained by molecular dynamic simulations, illustrating different intramolecular hydrogen bonds (green dots); type i (upper), type iii (middle), types i, ii & iii (below). The H atoms, except those of the NH groups, have been omitted for clarity.

In this context, the possible existence of the intramolecular hydrogen bonds within the molecules (**7c**), (**7d**), (**8c**), and (**8d**) was predicted using molecular dynamics calculations by applying the most favorable parameters for hydrogen bond formation on the 25 000 modelled structures (bond angle < 120° and the hydrogen bond distance < 3.2 Å).[49,58] In compound (**7c**), the calculations predicted the presence of two hydrogen bonds: (i) between CO (Boc) and the NH (azaPhe) of 2.86 Å closing a pseudocycle of 7 atoms, and (ii) between CO (azaPhe) and the $N^\varepsilon H$ (Lys2) of 2.96 Å closing a pseudocycle of 10 atoms, with occurrences of 36% and 35%, respectively, Table S3 (ESI†) and Fig. 4. Regarding compound (**7d**), the calculations indicated the possible existence of three hydrogen bonds: the first and second hydrogen bonds (i & ii) exist between the CO(Z) (Lys2) and both the NH (azaPhe) of 2.89 Å, and the NH (Lys1) of 2.91 Å, forming pseudocycles of 13 and 16 atoms, with occurrences of 40% and 26%, respectively. Based on molecular dynamic calculations, the disturbance from the classical βIV-turn in (**7c**) can be attributed to the involvement of the $N^\varepsilon H$ (Lys2) side chain

residue in intramolecular hydrogen bonds with either CO (azaPhe), or CO (Lys1), Fig. 4. Similarly, we observed a large deviation from the classical βI′-turn conformation particularly in the torsion angles ($\phi_1, \psi_1 = 128.40°, -64.24°$) for (**7d**), related to the possible existence of three intramolecular hydrogen bonds: (a) CO(Z)(Lys2) with NH (azaPhe), (b) CO(Z)(Lys2) with NH (D-Lys1), and (c) CO(Boc) with $N^\varepsilon H$ (D-Lys1), Fig. 5.
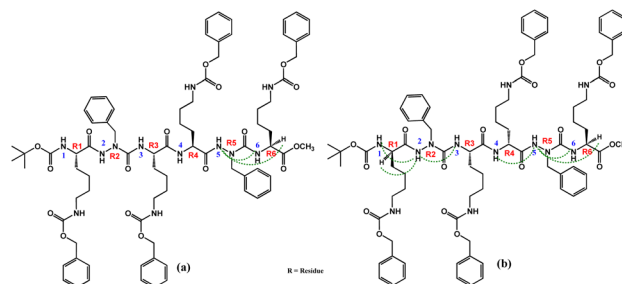

Fig. 6 ROE correlations of β-turn conformations in: (a) **8c**, and (b) **8d** (300 MHz, 4.0 mmol L^{-1}, $CDCl_3$, 300 K).

© 2023 The Author(s). Published by the Royal Society of Chemistry
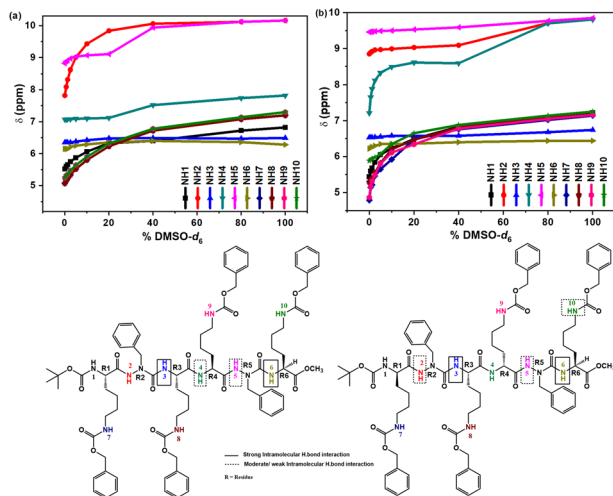
Fig. 7 Chemical shift-variations (δ) of NH protons for: (a) **8c**, and (b) **8d** as a function of % [CDCl$_3$/DMSO-d_6] mixtures.
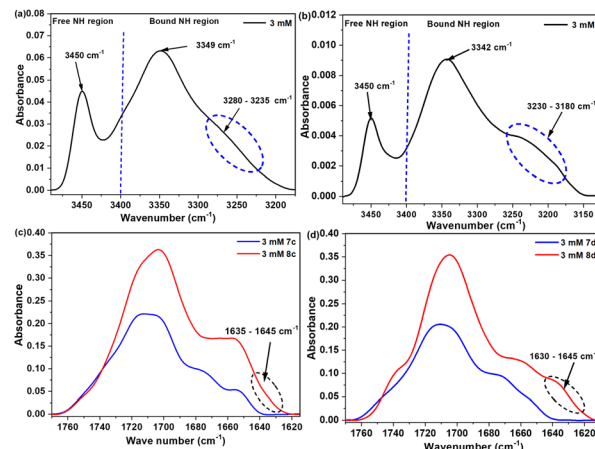

Fig. 8 FTIR spectra belong to the NH (up spectra), and CO (bottom spectra) stretching regions for: (a & c) **8c**, and (b & d) **8d** (3.0 mmol L^{-1}, CDCl$_3$).

NMR and FTIR spectroscopic studies of 2:1-[α/aza]-hexamers

^{1}H NMR studies for compounds (**8c**) and (**8d**) were carried out in CDCl$_3$ (4.0 mmol L^{-1}, 300 K). The ^{1}H spectrum of (**8d**) showed well resolved signals compared with the spectrum of (**8c**) (ESI, Fig. S7–S10†). The conformations favored by (**8c**) and (**8d**) in solution were investigated using 2D NMR (ROESY) experiments. Unfortunately, not many correlations in the ROE spectrum for compound (**8c**) were observed (ESI, Fig. S11†). Thus, it can be explained by the high steric hindrance between the four lysine side chains with the same S-configuration in (**8c**), allowing the molecule to be more flexible and hence adopting more energetically stable conformation, deviating from the classical β-turn conformation. Only the presence of weak correlation between C^{α}H (Lys4) and the NH (azaPhe2), and the moderate correlation between the NH (azaPhe2) and NH (Lys4) protons suggested that the C-terminal amino acid residues of compound **8c** might be folded in β-turn conformation, Fig. 6a.[30,49,57]

Concerning the solvent composition experiment by NMR technique, increasing the [DMSO-d_6/CDCl$_3$] mixture ratio showed that the NH1 (Lys1; **8c**) or (D-Lys1; **8d**) and all the NH protons of the lysine side chains (NH7–NH10; except NH10 of **8d**) for both compounds were very sensitive to the addition of DMSO-d_6 (ESI, Fig. S13†).

Accordingly, these protons are supposed to be free and not involved in intramolecular hydrogen bond due to their high sensitivity to [DMSO-d_6].[44] In contrast, the NH protons of the NH3 (Lys2) and NH6 (Lys4) of both compounds (**8c**) and (**8d**) were not sensitive to the addition of the DMSO-d_6 (Fig. 7). These findings suggested that these protons may be involved in strong intramolecular hydrogen bonds.[44]

For compound (**8c**), the NH2 (azaPhe1) is strongly affected by increasing % DMSO-d_6, which reflects the free state of this proton in solution (ESI, Fig. S13†), while NH4 (Lys3), and NH5 (azaPhe2) proton signals are not significantly shifted up to 20% DMSO-d_6, and more affected at higher DMSO-d_6

concentrations. These observations give indication that these NH protons are probably involved in weak intramolecular hydrogen bonds (Fig. 7a).[44] Concerning compound (**8d**), we observe (Fig. 7b) that the chemical shifts of the NH2 (azaPhe1) and NH5 (azaPhe2) protons are not affected by the addition of small amounts of DMSO-d_6, but are down-shielded by increasing the DMSO-d_6 concentration more than 40%, which indicates that these protons may be engaged in weak intramolecular hydrogen bonds (Fig. 7b). In contrast, the substantial change of the chemical shift of the NH4 (D-Lys3) upon gradual addition of DMSO-d_6 confirms that this proton is free and not involved in intramolecular hydrogen bonds (ESI, Fig. S13†). Interestingly, NH10 (Lys4) proton revealed weak dependency on % DMSO-d_6 till 5%, then its chemical shift acquired high values with increasing % DMSO-d_6, supposing the possibility of this NH10 (Lys4) proton to form a weak intramolecular hydrogen bond.

Similar to trimers, the IR spectra were recorded for hexamers (**8c**) and (**8d**) in dilute condition (3.0 mmol L^{-1}, CDCl$_3$). Both compounds (**8c** and **8d**) showed similar NH stretching regions as their trimers (**7c** and **7d**), respectively. The NH stretching region of both compounds demonstrates a band in the free NH region which assigned to the free NH protons. In addition, there was a very broad band in the bound NH region around 3345 cm^{-1} for both molecules, attributed to the bound NH protons of NH3 (Lys2) and NH6 (Lys4) (Fig. 8a and b). Interestingly, there is an additional broad band in the far NH stretching region (3235–3280 cm^{-1}) in (**8c**) and (3180–3230 cm^{-1}) in (**8d**) which were supposed to other intramolecular hydrogen bonds. Finally, one can notice that the bound NH bands in (**8d**) are more broadening with lower frequencies than those of the (**8c**), reflecting the presence of more number and stronger intramolecular hydrogen bonds in molecule (**8d**) than in (**8c**) (Fig. 8a and b). These results are consistent with the solvent composition studies by NMR technique.

Regarding the CO stretching domain, the two spectra are very similar to their trimers and they showed broadening and overlapping of the CO bands that caused an obstacle to assign all the bands even with the help of the 2nd derivative deconvolution method. By comparing the CO spectra of the trimer and the corresponding hexamer (Fig. 8c and d), both molecules (8c and 8d) exhibit new broad bands at (1635–1645 cm^{-1}) or (1630–1645 cm^{-1}), respectively which are characteristic of the presence of β-turn. These observations are consistent with the NMR studies, particularly for compound (8d). Based on the spectroscopic results, the NH3 (Lys2) and NH6 (Lys4) in compound (8d) are suggested to be involved in intramolecular hydrogen bonds with the CO (Boc) and CO (Lys3), respectively, stabilizing the two β-turns observed by the 2D ROESY in its two terminals, forming two pseudocycles of 10 atoms.

Analyses of the results obtained from the molecular dynamic simulations for the two hexamers (8c) and (8d) were more complicated than for their trimers (7c) and (7d). The complexity comes from the elongation of the backbone which increases the flexibility of the molecule to adopt the most stable energetically conformations. In addition, the presence of four lysine side chains in (8c) and (8d) competed in forming intramolecular hydrogen bonds with the amide groups of the main peptide chain and this may disturb the expected β-turn conformation in these oligomers. Based on the average values of the torsion angles for all the modelled 25 000 structures for the two oligomers (8c) and (8d) and comparing with the classical ones (ESI, Table S4†), the results suggested that: (a) Boc-[Lys(z)-azaPhe-Lys(z)]$_2$-OMe (8c) exists in equilibrium between several distorted β-turn conformations. Residues [1 & 2] show non-classical βV-turn conformation. On the other hand, residues [3 & 4] and [4 & 5] deviate from the classical βIV-turn conformation. Unexpectedly, residues [2/3] demonstrate distorted βII′- or βV′-turn since the β′-turn types were only reported for molecules possessing D-amino acids.[59] (b) Boc-[D-Lys(z)-azaPhe-Lys(z)]$_2$-OMe (8d) adopts mainly two consecutive distorted turns: βII′-turn between residues [2 & 3], and βI′-turn between residues [4 & 5]. (c) The deviation from the classical torsion angles values may be related to the involvement of the amide groups of the main backbone in non-classical β-turn intramolecular hydrogen bonds with either the amide groups of the main backbone and/or with the amide groups of the lysine side chains. These intramolecular hydrogen bonds affected the backbone dihedral angles leading to a deviation from the classical β-turn in natural peptides.

Accordingly, these results highlight that changing the chirality of the amino acid residues positioned at R1 and R4 from L-Lys in (8c) to D-Lys in (8d) reduces the flexibility of the molecule (8d) due to the presence of more hydrogen bond interactions, which by consequence adopts a more defined conformation in solution compared to compound (8c). This behavior of lysine side chain was previously reported stating the ability of the lysine residues to be involved in hydrogen bonds with residues elsewhere in the structure or with solvent molecules.[59] These results are consistent with the 2D NMR studies in solution as molecule (8c) shows weak correlations between the nuclei. Indeed, the molecule has no defined conformation in solution and exists in various conformations. In contrast, the strong correlation in the 2D spectrum of (8d) reflects that the molecule induces defined β-turns, as confirmed by molecular dynamic calculations.

Additionally, the Ptraj was employed for the analysis of the 25 000 structures for (8c) and (8d) to assess how the non-classical β-turn hydrogen bonds disturb the conformations adopted by the two molecules? The calculations for both molecules predicted several intramolecular hydrogen bonds as summarized in Table S5 (ESI†).

Briefly, in compound (8c), the calculations indicated the possibility of 4 different hydrogen bonds between: (i) CO (aza-Phe1) and NH (Lys3) closing a pseudocycle of 7 atoms occurring at 90% of the modelled frames; (ii) CO (Lys1) and N$^\varepsilon$H (Lys3) closing a pseudoring of 16 atoms with 64.9%; (iii) CO (Boc) and NH (azaPhe1) closing a pseudocycle of 7 atoms with 48.9%; and (iv) CO (azaPhe1) and NH (azaPhe2) closing a pseudocycle of 10 atoms with occurrence of 32.9%. The calculations for compound (8d) predicted the possibility of 6 different hydrogen bonds. The hydrogen bonds are: (i) CO (D-Lys1) and NH (aza-Phe5) closing a pseudocycle of 13 atoms occurring as 59.1% of the modelled frames, (ii) CO(Z) (Lys4) and NH (D-Lys1) closing a pseudoring of 25 atoms with 58.7%; (iii) CO (azaPhe1) and NH (D-Lys3) closing a pseudocycle of 7 atoms with occurrence of 38.9%; (iv) (CO$_i$) Boc and NH$_{i+2}$ (azaPhe1) closing a pseudocycle of 7 atoms with 29.5%; (v) CO(Z) (D-Lys3) and N$^\varepsilon$H (D-Lys1) closing a pseudocycle of 23 atoms with occurrence of 26.9%; and (vi) CO (azaPhe2) and N$^\varepsilon$H (Lys2) closing a pseudocycle of 12 atoms with occurrence of 23.0%.

These results are consistent with NMR results in solution which supposed that the protons of NH4 and NH5 are involved in weak hydrogen bonds in the case of (8c). Similarly, the protons NH2 and NH5 in compound (8d) may be engaged in weak intramolecular hydrogen bonds at low % DMSO-d_6.

In addition, the modelling calculations interpreted the observed broad NH bound bands in the FTIR spectra for both molecules due to the presence of several hydrogen bonds as confirmed by molecular dynamic calculations. Moreover, by applying the most favorable parameters for hydrogen bond formation,[49,58] the calculations gave an idea related to the average percentages for the predicted intramolecular hydrogen bonds in both molecules (ESI, Tables S6 and S7†). Examples for a number of selected frames with more than one hydrogen bond representing molecules 8c and 8d are shown in Fig. 9 and 10, respectively.

Application as additives in polymeric membranes for CO_2 capture

In this work, we have investigated a selection of the synthesized azapeptides as bio-based additives in an original non-medical application, the CO_2 membrane separation (Fig. 11). If anti-bacterial peptides have been reported for a long time to limit biofouling for water treatment membranes, recent promising works have shown the high potential of peptides and polypeptides for increasing water permeability of dialysis, water purification and nanofiltration membranes.[60–65] However, the
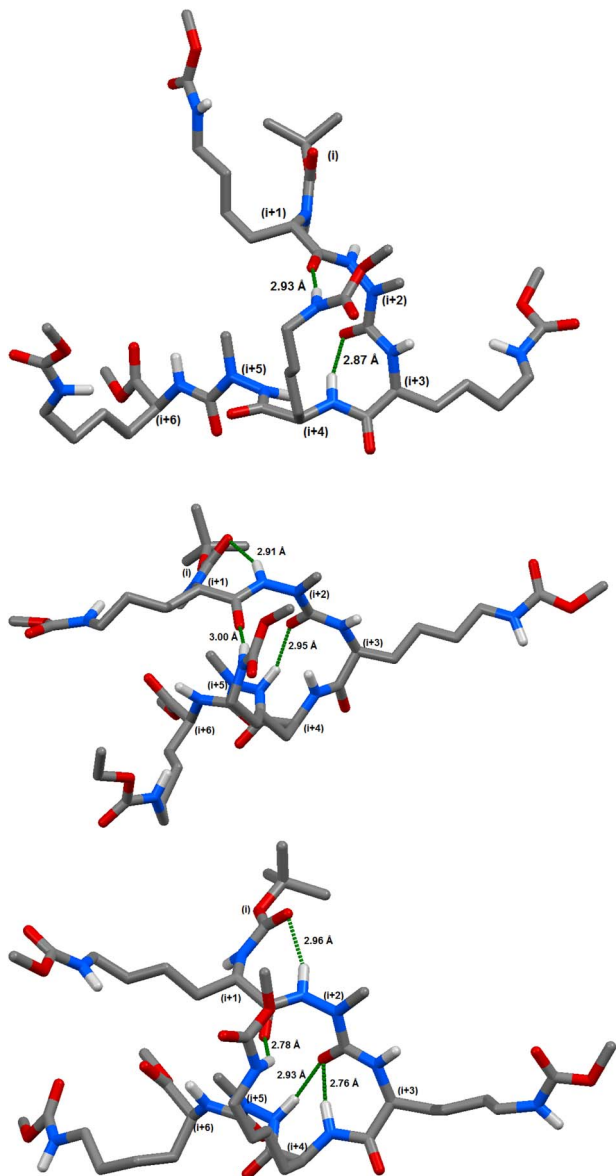
Fig. 9 Selected frames for molecule (**8c**) obtained by molecular dynamic simulations, illustrating different intramolecular hydrogen bonds (green dots). The H atoms, except those of the NH groups, and the phenyl groups have been omitted for clarity.
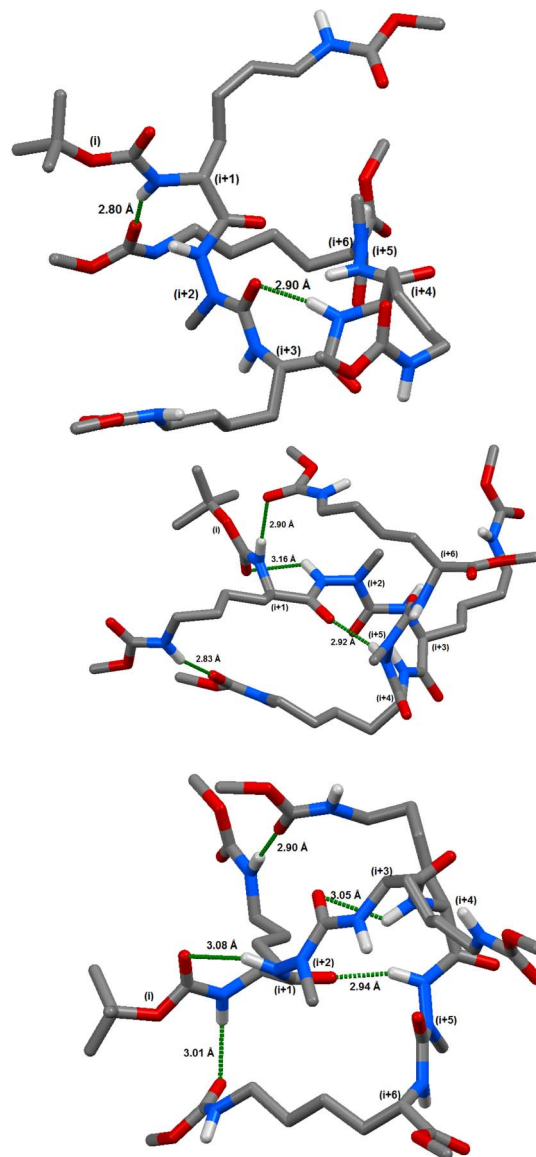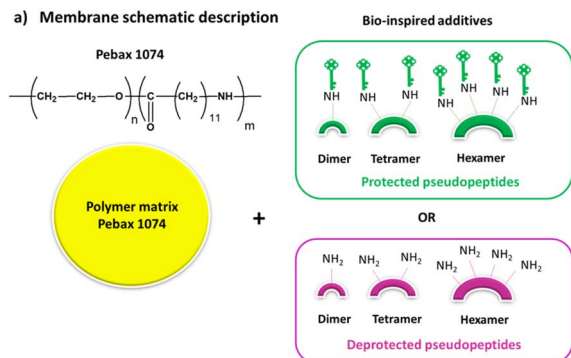

Fig. 10 Selected frames for molecule (**8d**) obtained by molecular dynamic simulations, illustrating different intramolecular hydrogen bonds (green dots). The H atoms, except those of the NH groups, and the phenyl groups have been omitted for clarity.

use of peptides or pseudopeptides for CO_2 separation membranes has remained an almost unexplored field so far. In 2016, we have reported the first work on pseudopeptide additives and their corresponding bioconjugates with a CO_2-philic polymeric part for greatly improving CO_2 permeability through CO_2 separation membranes.[55] In 2019, Prasad *et al.* have used sericin polypeptide (*i.e.* a waste product of the silk industry) as additive in chitosan membranes for CO_2 separations.[66] At high temperatures (80–100 °C), one of these polypeptide-based membranes had CO_2/N_2 separation performances above the 2008 Robeson upper-bound. Furthermore, amino acids have also been used in bio-based ionic liquids (ILs) or poly(ionic liquid)s (PILs) for CO_2 absorption processes.[67–69] These former

works have shown that the ILs or PILs derived from amino acids containing an amine side group (*e.g.*, lysine or arginine) were performing better than the non-functional ILs or PILs. The strong interactions of CO_2 with the free amine groups were responsible for better CO_2 absorption performances. The presence of free amine groups is also responsible for the very high performance of several facilitated transport membranes for CO_2 separations.[70,71] The different reactions of amines with CO_2 are quite complex and depend on the amine structure and on the operating conditions (absence or presence of water).[72–74] Fig. 11 shows the different membranes with the new bio-based additives for CO_2 separation and the main related reactions between primary amine groups and CO_2 for the deprotected additives. According to Ben Said *et al.*, the main reaction of primary

Fig. 12 Ideal selectivity α_{CO_2/N_2} as function of CO_2 permeability (Robeson plot) for different Pebax® 1074 membranes with protected and deprotected pseudopeptide additives at 2 bar and 35 °C.
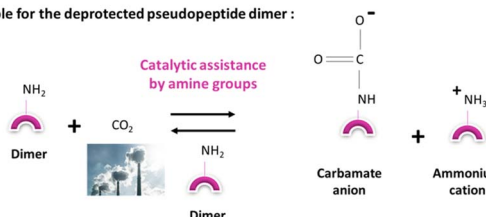
Fig. 11 (a) The different membranes with the new bio-inspired additives for CO_2 separation targeting CO_2 post-combustion capture, and (b) the main reaction of the deprotected bio-inspired additives with CO_2.

Table 2 Description of the aza-pseudopeptide oligomers tested as additives in Pebax® 1074 membrane for CO_2 capture

ID	Pseudopeptide oligomer	No. of lysine residue(s)	Lysine residue(s)
6b	Dimer	1	Protected
6b′[a]		1	Free
7a	Trimer	0	—
7c		2	Protected
7c′[a]		2	Free
8c	Hexamer	4	Protected
8c′[a]		4	Free

[a] Deprotected azapeptides **6b′**, **7c′** and **8c′** were obtained from the corresponding protected analogues by catalytic hydrogenolysis (see Experimental section).

amines with CO_2 proceeds through catalytic assistance by amine (or water if any) to form a carbamate anion and an ammonium cation.[72] This reaction is reversible and can thus give back amine and CO_2.

In this work, seven aza-pseudopeptide oligomers (**6b, 6b′, 7a, 7c, 7c′, 8c,** and **8c′**) from the synthesized 2:1-[α/aza]-series (Table 2) were tested as additives in Pebax® 1074 membrane, already known for its good performance for CO_2 capture[55,75,76] (ESI, Fig. S14†). These pseudopeptide oligomers differed in their length (from dimer to hexamer oligomers) and the type of their side group. In a first series of protected pseudopeptide oligomers, the amine side group of the lysine residue was protected with a carboxybenzyl (Z) group. In a second series of
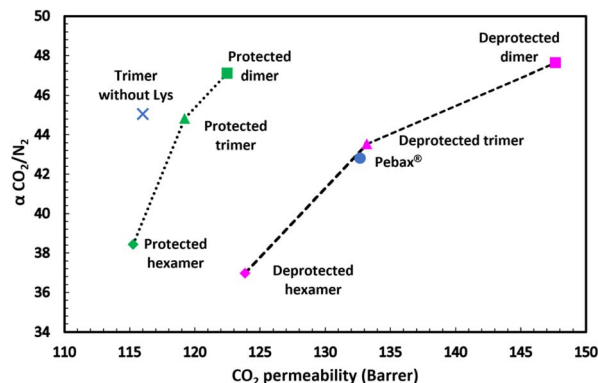
deprotected pseudopeptide oligomers, this amine side group was deprotected. For comparison, a pseudopeptide trimer without lysine residue was also tested to assess the influence of this charged amino acid on the gas permeation properties. The results of the membrane permeation properties for CO_2 and N_2 pure gases are reported in Table S8 (ESI†).

Fig. 12 shows the ideal selectivity α_{CO_2/N_2} as a function of CO_2 permeability (Robeson plot) for the different membranes at 2 bar and 35 °C, which are typical conditions for CO_2 capture. The protected pseudopeptide trimer with lysine residues and the deprotected pseudopeptide trimer had better CO_2 permeability compared to the corresponding trimer without lysine residue, showing the positive effect of the lysine for CO_2 permeation.
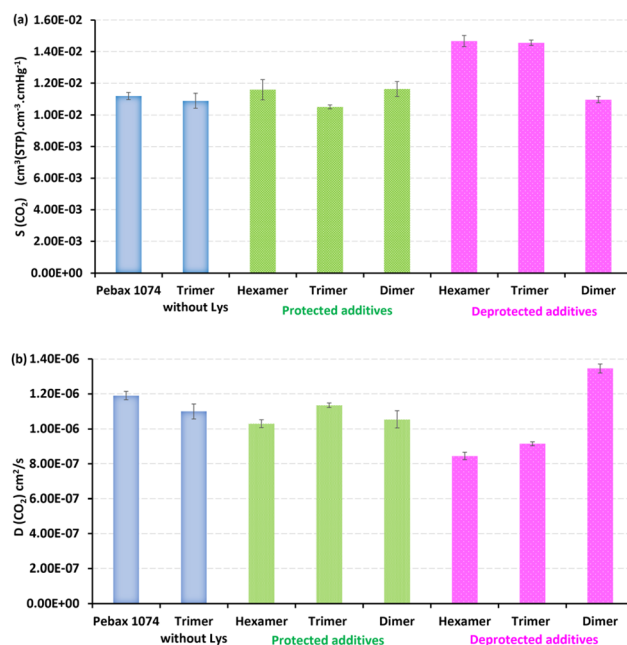

Fig. 13 CO_2 sorption (a) and diffusion (b) coefficients for different Pebax® 1074 membranes with protected and deprotected pseudopeptide additives at 2 bar and 35 °C.

For both series of pseudopeptide oligomers, both the ideal selectivity and the CO_2 permeability decrease when the pseudopeptide oligomer length increases from dimer to hexamer, and this effect was reinforced for the deprotected pseudopeptide oligomers (Fig. 12). The deprotection of the pseudopeptide oligomer leads to free amine side group for the lysine residue(s), resulting in a systematic improvement of the CO_2 permeability. It is well known that free amines have strong ability to interact with CO_2 and the incorporation of amine-based additives in polymer membranes usually improves CO_2 permeability.[69,77–81] In this work, the extent of this improvement increases when the pseudopeptide oligomer length decreases. Therefore, the best membrane properties were obtained for the deprotected pseudopeptide dimer, overcoming the usual selectivity/permeability trade-off[82–84] with an increase in both ideal selectivity α_{CO_2/N_2} (from 42.8 to 47.6) and CO_2 permeability (from 132 to 148 Barrer) compared to the virgin Pebax® 1074 membrane.

The CO_2 sorption coefficients obtained for the membranes with the different protected pseudopeptide additives were very close to each other and also to that of the virgin Pebax® 1074 membrane, meaning that the protected pseudopeptide additives did not have any significant effect on the sorption step during CO_2 permeation (Fig. 13). However, as expected, the deprotected pseudopeptide additives led to higher CO_2 sorption coefficients and the best sorption improvement was obtained for the deprotected hexamer, *i.e.* the longest pseudopeptide oligomer containing four deprotected lysine residues. The four corresponding free amine side groups strongly interacted with the CO_2 molecules and increased CO_2 sorption by 30%. This result is in good agreement with former works ILs and PILs based on amino acids, having shown the good interactions of CO_2 molecules with free amine side groups of lysine or arginine amino acids.[67–69] The different protected pseudopeptide additives induce a very low reduction in the CO_2 diffusion coefficient partially due to the presence of the bulky carboxybenzyl (Z) protecting group slightly limiting the diffusion of CO_2 molecules (Fig. 13).

However, the CO_2 diffusion coefficient was decreased by 23% and 30% for the deprotected trimer and hexamer additives, respectively, compared to that obtained with the virgin Pebax® 1074 membrane. On the other hand, the CO_2 diffusion coefficient slightly increased (+13%) for the deprotected dimer additive. Therefore, the deprotected pseudopeptide length has a strong effect on the CO_2 diffusion coefficient, the longest additives hindering CO_2 diffusion. It has been shown in the first part of this work that increasing the length of the pseudopeptide oligomers favors their structuration by involving more and more β-turn conformations when going from dimer to trimer and hexamer. For the series of deprotected pseudopeptide additives, the best CO_2 diffusion coefficient was obtained for the less structured pseudopeptide oligomer (dimer).

To conclude the gas permeation results, the deprotected pseudopeptide trimer and hexamer additives improve CO_2 sorption, the best improvement being obtained for the hexamer additive containing four lysine residues and four free amine side groups. The deprotected pseudopeptide dimer additive did not have any significant effect on CO_2 sorption compared to that of the virgin Pebax® 1074 membrane. However, the strong structuration of the long deprotected additives induces a strong decrease of the CO_2 diffusion coefficient, finally resulting in a decrease in CO_2 permeability. Nevertheless, the low structuration of the deprotected dimer additive led to higher CO_2 diffusion coefficient (+13%), finally resulting in higher membrane CO_2 permeability (+12%) and better ideal selectivity α_{CO_2/N_2} (+11%) compared to virgin Pebax 1074. The best CO_2 permeability (148 Barrer) and ideal selectivity (47.6) obtained in this work with the new deprotected dimer additive are very close to those reported in our first work on other pseudopeptide bio-inspired additives in Pebax 1074 membranes for CO_2 separation in the same operating conditions (pressure: 2 bar, temperature: 35 °C).[55] Furthermore, in the former work, a dimer pseudopeptide was also better performing than the corresponding tetramer, due its lower structuration.

Conclusions

The work provided a comprehensive study on the synthesis, characterizations, and conformational studies of a new series of 2:1-[α/aza]-oligomers (trimers and hexamers) incorporating lysine amino acid residue, besides their potentiality in gases separation application. The influence of the $N^\varepsilon H$ on the conformation of these oligomers were established using NMR, FTIR and molecular dynamic calculations. The spectroscopy techniques emphasized the adoption of the β-turn conformations regardless the chirality and side chain of lysine particularly in small sequence, while the chirality and chain length exerted their role in β-turn deviation. On the other hand, molecular dynamic simulations predicted the impact of the supplementary $N^\varepsilon H$ of the lysine residue and of the chain length on the backbone torsion angles, highlighting the presence of intramolecular hydrogen bonds with the amide groups of the azapeptide backbone, causing distortion from the classical β-turn particularly in longer sequences (hexamers < trimers). In addition, increasing the chain length (hexamer) and the high steric hindrance caused by the four lysine residues (**8c** < **8d**) led to increasing the flexibility of the hexamers to fold into more energetically stable conformation stabilized by non-classical β-turn hydrogen bonds. Furthermore, to the best of our knowledge, so far, the use of bio-inspired pseudopeptide additives for CO_2 separation membranes has only been reported by our team in a single work in 2016. In this new study, the synthesized short azapeptide based lysine moiety with free amine side chain (deprotected dimer) exerted a good improvement in CO_2 separation upon using them as additive in Pebax® matrix membrane. In the future, more molecular dynamics simulations in explicit membrane environment would be an interesting to investigate in order to decipher more precisely the peptide structure/membrane properties. Additionally, following our related work on the first bio-inspired pseudopeptide additives for CO_2 separation membranes,[55] the new deprotected dimer could be used for developing new bioconjugates based on CO_2-philic oligomers for further improving membrane properties for CO_2 separations including CO_2 post-combustion capture for preventing the associated global climatic changes.

Author contributions

Conflicts of interest

There are no conflicts to declare.

Acknowledgements

Notes and references

1 I. Avan, C. D. Hall and A. R. Katritzky, Peptidomimetics *via* modifications of amino acids and peptide bonds, *Chem. Soc. Rev.*, 2014, **43**, 3575–3594, DOI: **10.1039/C3CS60384A**.

2 G. Cardillo, L. Gentilucci and A. Tolomelli, Aziridines and Oxazolines: Valuable Intermediates in the Synthesis of Unusual Amino Acids, Universita di Bologna, *Aldrichim Acta*, 2003, **36**, 39–50, **https://www.sigmaaldrich.com/JP/en/collections/aldrichimica-acta**.

3 A. Perdih, M. Sollner Dolenc, *Current Organic Chemistry: Recent Advances in the Synthesis of Unnatural α-Amino Acids*, Bentham Science Publishers, 2007, vol. 11, pp. 801–832, DOI: **10.2174/138527207780831701**.

4 A. Azam, S. Mallart, S. Illiano, O. Duclos, C. Prades and B. Maillère, Introduction of Non-natural Amino Acids Into T-Cell Epitopes to Mitigate Peptide-Specific T-Cell Responses, *Front. Immunol.*, 2021, **12**, DOI: **10.3389/fimmu.2021.637963**.

5 G. Cardillo, L. Gentilucci and A. Tolomelli, Unusual amino acids: synthesis and introduction into naturally occurring peptides and biologically active analogues, *Mini-Rev. Med. Chem.*, 2006, **6**, 293–304, DOI: **10.2174/138955706776073394**.

6 A. Dahal, J. J. Sonju, K. G. Kousoulas and S. D. Jois, Peptides and peptidomimetics as therapeutic agents for Covid-19, *Pept. Sci.*, 2022, **114**, e24245, DOI: **10.1002/pep2.24245**.

7 N. Sewald, H.-D. Jakubke, *Peptide Synthesis in Peptides: Chemistry and Biology*, Wiley-VCH Verlag GmbH & Co. KGaA, 2002, pp. 339–361, DOI: **10.1002/352760068X**.

8 J. V. N. Vara Prasad and D. H. Rich, Addition of Allylic Metals to α-Aminoaldehydes. Application to the Synthesis of Statine, Ketomethylene and Hydroxyethylene Dipeptide Isosteres, *Tetrahedron Lett.*, 1990, **31**, 1803–1806, DOI: **10.1016/S0040-4039(00)98790-2**.

9 J. Gante, Azapeptides, *Synthesis*, 1989, **21**, 405–413, DOI: **10.1055/s-1989-27269**.

10 J. Magrath and R. H. Abeles, Cysteine protease inhibition by azapeptide esters, *J. Med. Chem.*, 1992, **35**, 4279–4283, DOI: **10.1021/jm00101a004**.

11 M. Chorev and M. Goodman, A dozen years of retro-inverso peptidomimetics, *Acc. Chem. Res.*, 1993, **26**, 266–273, DOI: **10.1021/ar00029a007**.

12 L. Thévenet, R. Vanderesse, M. Marraud, C. Didierjean and A. Aubry, Pseudopeptide fragments and local structures induced by an α-aminoxy acid in a dipeptide, *Tetrahedron Lett.*, 2000, **41**, 2361–2364, DOI: **10.1016/S0040-4039(00)00200-8**.

13 D. Yang, J. Qu, B. Li, F.-F. Ng, X.-C. Wang, K.-K. Cheung, D.-P. Wang and Y.-D. Wu, Novel Turns and Helices in Peptides of Chiral α-Aminoxy Acids, *J. Am. Chem. Soc.*, 1999, **121**, 589–590, DOI: **10.1021/ja982528y**.

14 A. Aubry, J.-P. Mangeot, J. Vidal, A. Collet, S. Zerkout and M. Marraud, Crystal structure analysis of a β-turn mimic in hydrazino peptides, *Int. J. Pept. Protein Res.*, 1994, **43**, 305–311, DOI: **10.1111/j.1399-3011.1994.tb00395.x**.

15 A. Cheguillaume, F. Lehardy, K. Bouget, M. Baudy-Floc'h and P. Le Grel, Submonomer Solution Synthesis of Hydrazinoazapeptoids, a New Class of Pseudopeptides, *J. Org. Chem.*, 1999, **64**, 2924–2927, DOI: **10.1021/jo981487l**.

16 A. Müller, C. Vogt and N. Sewald, Synthesis of Fmoc-β-Homoamino Acids by Ultrasound-Promoted Wolff Rearrangement, *Synthesis*, 1998, **1998**, 837–841, DOI: **10.1055/s-1998-2075**.

17 S. H. Gellman, Foldamers: A Manifesto, *Acc. Chem. Res.*, 1998, **31**, 173–180, DOI: **10.1021/ar960298r**.

18 F. André, G. Boussard, D. Bayeul, C. Didierjean, A. Aubry and M. Marraud, Aza-peptides. II. X-ray structures of aza-alanine and aza-asparagine-containing peptides, *J. Pept. Res.*, 1997, **49**, 556–562, DOI: **10.1111/j.1399-3011.1997.tb01163.x**.

19 R. Vanderesse, V. Grand, D. Limal, A. Vicherat, M. Marraud, C. Didierjean and A. Aubry, Structural Comparison of Homologous Reduced Peptide, Reduced Azapeptide, Iminoazapeptide, and Methyleneoxypeptide Analogues, *J. Am. Chem. Soc.*, 1998, **120**, 9444–9451, DOI: **10.1021/ja980937o**.

20 M. I. A. Ibrahim, G. Pickaert, L. Stefan, B. Jamart-Grégoire, J. Bodiguel and M.-C. Averlant-Petit, Cyclohexamer [-(d-Phe-azaPhe-Ala)2-]: good candidate to formulate supramolecular organogels, *RSC Adv.*, 2020, **10**, 43859–43869, DOI: **10.1039/D0RA07775E**.

21 A. Lecoq, G. Boussard, M. Marraud and A. Aubry, The couple Pro/AzaPro: A means of β-turn formation control synthesis and conformation of two AzaPro-containing dipeptides,

Tetrahedron Lett., 1992, **33**, 5209–5212, DOI: **10.1016/S0040-4039(00)79134-9**.

22 I. Bouillon, N. Brosse, R. Vanderesse and B. Jamart-Grégoire, Synthesis of Nα-Z, Nβ-Fmoc or Boc protected α-hydrazinoacids and study of the coupling reaction in solution of Nα-Z-α-hydrazinoesters, *Tetrahedron*, 2007, **63**, 2223–2234, DOI: **10.1016/j.tet.2006.12.085**.

23 I. Bouillon, R. Vanderesse, N. Brosse, O. Fabre and B. Jamart-Grégoire, Solid-phase synthesis of hydrazinopeptides in Boc and Fmoc strategies monitored by HR-MAS NMR, *Tetrahedron*, 2007, **63**, 9635–9641, DOI: **10.1016/j.tet.2007.07.038**.

24 A.-S. Felten, S. Dautrey, J. Bodiguel, R. Vanderesse, C. Didierjean, A. Arrault and B. Jamart-Grégoire, Oligomerization of N-aminodipeptides: to the synthesis of heterogeneous backbone with 1:1 α:α-N-amino aminoacid residue patterns, *Tetrahedron*, 2008, **64**, 10741–10753, DOI: **10.1016/j.tet.2008.08.087**.

25 R.-O. Moussodia, S. Acherar, A. Bordessa, R. Vanderesse and B. Jamart-Grégoire, An expedient and short synthesis of chiral α-hydrazinoesters: synthesis and conformational analysis of 1:1 [α/α-Nα-hydrazino]mers, *Tetrahedron*, 2012, **68**, 4682–4692, DOI: **10.1016/j.tet.2012.04.018**.

26 A.-S. Felten, R. Vanderesse, N. Brosse, C. Didierjean and B. Jamart-Grégoire, Solid phase synthesis of N-aminodipeptides in high optical purity, *Tetrahedron Lett.*, 2008, **49**, 156–158, DOI: **10.1016/j.tetlet.2007.10.152**.

27 M. I. A. Ibrahim, Z. Zhou, C. Deng, C. Didierjean, R. Vanderesse, J. Bodiguel, M.-C. Averlant-Petit and B. Jamart-Grégoire, Impact of Cα-Chirality on Supramolecular Self-Assembly in Cyclo-2:1-[α/aza]-Hexamers (d/l-Phe-azaPhe-Ala)2, *Eur. J. Org. Chem.*, 2017, **2017**, 4703–4712, DOI: **10.1002/ejoc.201700555**.

28 N. Brosse, A. Grandeury and B. Jamart-Grégoire, Original and efficient method for the preparation of N-aminoamide pseudodipeptides in high optical purity, *Tetrahedron Lett.*, 2002, **43**, 2009–2011, DOI: **10.1016/S0040-4039(02)00119-3**.

29 C. Abbas, B. Jamart Gregoire, R. Vanderesse and C. Didierjean, Boc-AzAla-Ala-OMe, *Acta Crystallogr., Sect. E: Struct. Rep. Online*, 2009, **65**, o3079, DOI: **10.1016/j.tetlet.2009.04.131**.

30 Z. Zhou, C. Deng, C. Abbas, C. Didierjean, M.-C. Averlant-Petit, J. Bodiguel, R. Vanderesse and B. Jamart-Grégoire, Synthesis and Structural Characterization of 2:1 [α/Aza]-oligomers, *Eur. J. Org. Chem.*, 2014, **2014**, 7643–7650, DOI: **10.1002/ejoc.201402628**.

31 C. Abbas, G. Pickaert, C. Didierjean, B. J. Gregoire and R. Vanderesse, Original and efficient synthesis of 2:1-[α/aza]-oligomer precursors, *Tetrahedron Lett.*, 2009, **50**, 4158–4160, DOI: **10.1016/j.tetlet.2009.04.131**.

32 M. Marraud and A. Aubry, Crystal structures of peptides and modified peptides, *Biopolymers*, 1996, **40**, 45–83, DOI: **10.1002/(sici)1097-0282(1996)40:1<45::aid-bip3>3.0.co;2-3**.

33 J. Gante, Peptidomimetics—Tailored Enzyme Inhibitors, *Angew. Chem., Int. Ed. Engl.*, 1994, **33**, 1699–1720, DOI: **10.1002/anie.199416991**.

34 J. Gante, M. Krug, G. Lauterbach, R. Weitzel and W. Hiller, Synthesis and properties of the first all-aza analogue of a biologically active peptide, *J. Pept. Sci.*, 1995, **1**, 201–206, DOI: **10.1002/psc.310010307**.

35 K. Fan Cheng, S. VanPatten, M. He and Y. Al-Abed, Azapeptides -A History of Synthetic Milestones and Key Examples, *Curr. Med. Chem.*, 2022, **29**, 6336–6358, DOI: **10.2174/0929867329666220510214402**.

36 A. S. Dutta and J. S. Morley, Polypeptides. Part XIII. Preparation of α-aza-amino-acid (carbazic acid) derivatives and intermediates for the preparation of α-aza-peptides, *J. Chem. Soc., Perkin Trans. 1*, 1975, **1**, 1712–1720, DOI: **10.1039/p19750001712**.

37 Z. Benatalah, A. Aubry, G. Boussard and M. Marraud, Evidence for a beta-turn in an azadipeptide sequence. Synthesis and crystal structure of ButCO-Pro-AzaAla-NHPri, *Int. J. Pept. Protein Res.*, 1991, **38**, 603–605, DOI: **10.1111/j.1399-3011.1991.tb01547.x**.

38 C. J. Gray, M. Quibell, N. Baggett and T. Hammerle, Incorporation of azaglutamine residues into peptides synthesised by the ultra-high load solid (gel)-phase technique, *Int. J. Pept. Protein Res.*, 1992, **40**, 351–362, DOI: **10.1111/j.1399-3011.1992.tb00311.x**.

39 E. Benedetti, Structure and conformation of peptides: a critical analysis of crystallographic data, in *Peptides proceedings of fifth american peptide symposium*, ed. M. Goodman and J. Meienhofer, Wiley, 1977, pp. 257–273.

40 C. H. Reynolds and R. E. Hormann, Theoretical Study of the Structure and Rotational Flexibility of Diacylhydrazines: Implications for the Structure of Nonsteroidal Ecdysone Agonists and Azapeptides, *J. Am. Chem. Soc.*, 1996, **118**, 9395–9401, DOI: **10.1021/ja960214+**.

41 H.-J. Lee, M.-H. Lee, Y.-S. Choi, H.-M. Park and K.-B. Lee, NBO approach to evaluate origin of rotational barrier of diformylhydrazine, *J. Mol. Struct.: THEOCHEM*, 2003, **631**, 101–110, DOI: **10.1016/S0166-1280(03)00191-X**.

42 C. Proulx, D. Sabatino, R. Hopewell, J. Spiegel, Y. García Ramos and W. D. Lubell, Azapeptides and their therapeutic potential, *Future Med. Chem.*, 2011, **3**, 1139–1164, DOI: **10.4155/fmc.11.74**.

43 H. J. Lee, I. A. Ahn, S. Ro, K. H. Choi, Y. S. Choi and K. B. Lee, Role of azaamino acid residue in beta-turn formation and stability in designed peptide, *J. Pept. Res.*, 2000, **56**, 35–46, DOI: **10.1034/j.1399-3011.2000.00717.x**.

44 F. André, A. Vicherat, G. Boussard, A. Aubry and M. Marraud, Aza-peptides. III. Experimental structural analysis of aza-alanine and aza-asparagine-containing peptides, *J. Pept. Res.*, 1997, **50**, 372–381, DOI: **10.1111/j.1399-3011.1997.tb01197.x**.

45 M. Zouikri, A. Vicherat, A. Aubry, M. Marraud and G. Boussard, Azaproline as a beta-turn-inducer residue opposed to proline, *J. Pept. Res.*, 1998, **52**, 19–26, DOI: **10.1111/j.1399-3011.1998.tb00648.x**.

46 H. J. Lee, K. H. Choi, I. A. Ahn, S. Ro, H. G. Jang, Y. S. Choi and K. B. Lee, The β-turn preferential solution conformation of a tetrapeptide containing an azaamino acid residue, *J.*
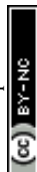
Mol. Struct., 2001, **569**, 43–54, DOI: 10.1016/S0022-2860(00)00861-9.

47 C. Didierjean, V. Del Duca, E. Benedetti, A. Aubry, M. Zouikri, M. Marraud and G. Boussard, X-ray structures of aza-proline-containing peptides, *J. Pept. Res.*, 1997, **50**, 451–457, DOI: 10.1111/j.1399-3011.1997.tb01208.x.

48 A. Lecoq, G. Boussard, M. Marraud and A. Aubry, Crystal state conformation of three azapeptides containing the Azaproline residue, a β-turn regulator, *Biopolymers*, 1993, **33**, 1051–1059, DOI: 10.1002/bip.360330707.

49 M. Thormann and H.-J. Hofmann, Conformational properties of azapeptides, *J. Mol. Struct.: THEOCHEM*, 1999, **469**, 63–76, DOI: 10.1016/S0166-1280(98)00567-3.

50 H.-J. Lee, J.-W. Song, Y.-S. Choi, S. Ro and C.-J. Yoon, The energetically favorable cis peptide bond for the azaglycine-containing peptide: For-AzGly-NH2 model, *Phys. Chem. Chem. Phys.*, 2001, **3**, 1693–1698, DOI: 10.1039/B009651M.

51 W.-J. Zhang, A. Berglund, J. L. F. Kao, J.-P. Couty, M. C. Gershengorn and G. R. Marshall, Impact of Azaproline on Amide Cis–Trans Isomerism: Conformational Analyses and NMR Studies of Model Peptides Including TRH Analogues, *J. Am. Chem. Soc.*, 2003, **125**, 1221–1235, DOI: 10.1021/ja020994o.

52 H. J. Lee, J. W. Song, Y. S. Choi, H. M. Park and K. B. Lee, A theoretical study of conformational properties of N-methyl azapeptide derivatives, *J. Am. Chem. Soc.*, 2002, **124**, 11881–11893, DOI: 10.1021/ja026496x.

53 D. A. Case, T. E. Cheatham III, T. Darden, H. Gohlke, R. Luo, K. M. Merz Jr, A. Onufriev, C. Simmerling, B. Wang and R. J. Woods, The Amber biomolecular simulation programs, *J. Comput. Chem.*, 2005, **26**, 1668–1688, DOI: 10.1002/jcc.20290.

54 D. A. Pearlman, D. A. Case, J. W. Caldwell, W. S. Ross, T. E. Cheatham, S. DeBolt, D. Ferguson, G. Seibel and P. Kollman, AMBER, a package of computer programs for applying molecular mechanics, normal mode analysis, molecular dynamics and free energy calculations to simulate the structural and energetic properties of molecules, *Comput. Phys. Commun.*, 1995, **91**, 1–41, DOI: 10.1016/0010-4655(95)00041-D.

55 X. Solimando, C. Lherbier, J. Babin, C. Arnal-Herault, E. Romero, S. Acherar, B. Jamart-Gregoire, D. Barth, D. Roizard and A. Jonquieres, Pseudopeptide bioconjugate additives for CO2 separation membranes, *Polym. Int.*, 2016, **65**, 1464–1473, DOI: 10.1002/pi.5240.

56 J. G. Wijmans and R. W. Baker, The solution-diffusion model: a review, *J. Membr. Sci.*, 1995, **107**, 1–21, DOI: 10.1016/0376-7388(95)00102-I.

57 H.-J. Lee, H.-M. Park and K.-B. Lee, The β-turn scaffold of tripeptide containing an azaphenylalanine residue, *Biophys. Chem.*, 2007, **125**, 117–126, DOI: 10.1016/j.bpc.2006.05.028.

58 J. J. Dannenberg, An Introduction to Hydrogen Bonding By George A. Jeffrey (University of Pittsburgh). Oxford University Press: New York and Oxford. 1997. ix + 303 pp. $60.00. ISBN 0-19-509549-9, *J. Am. Chem. Soc.*, 1998, **120**, 5604, DOI: 10.1021/ja9756331.

59 R. P. Cheng, P. Girinath and R. Ahmad, Effect of lysine side chain length on intra-helical glutamate–lysine ion pairing interactions, *Biochemistry*, 2007, **46**, 10528–10537, DOI: 10.1021/bi700701z.

60 S. Bolisetty and R. Mezzenga, Amyloid–carbon hybrid membranes for universal water purification, *Nat. Nanotechnol.*, 2016, **11**, 365–371, DOI: 10.1038/nnano.2015.310.

61 Y. He, H. Hoi, C. D. Montemagno and S. Abraham, Functionalized polymeric membrane with aquaporin using click chemistry for water purification application, *J. Appl. Polym. Sci.*, 2018, **135**, 46678, DOI: 10.1002/app.46678.

62 C. S. Lee, M.-k. Choi, Y. Y. Hwang, H. Kim, M. K. Kim and Y. J. Lee, Facilitated Water Transport through Graphene Oxide Membranes Functionalized with Aquaporin-Mimicking Peptides, *Adv. Mater.*, 2018, **30**, 1705944, DOI: 10.1002/adma.201705944.

63 B. Sutisna, P. Bilalis, V. Musteata, D.-M. Smilgies, K.-V. Peinemann, N. Hadjichristidis and S. P. Nunes, Self-Assembled Membranes with Featherlike and Lamellar Morphologies Containing α-Helical Polypeptides, *Macromolecules*, 2018, **51**, 8174–8187, DOI: 10.1021/acs.macromol.8b01446.

64 S. Schöttner, M. Brodrecht, E. Uhlein, C. Dietz, H. Breitzke, A. A. Tietze, G. Buntkowsky and M. Gallei, Amine-Containing Block Copolymers for the Bottom-Up Preparation of Functional Porous Membranes, *Macromolecules*, 2019, **52**, 2631–2641, DOI: 10.1021/acs.macromol.8b02758.

65 X. Niu, D. Li, Y. Chen and F. Ran, Modification of a polyethersulfone membrane with a block copolymer brush of poly(2-methacryloyloxyethyl phosphorylcholine-co-glycidyl methacrylate) and a branched polypeptide chain of Arg–Glu–Asp–Val, *RSC Adv.*, 2019, **9**, 25274–25284, DOI: 10.1039/C9RA04234B.

66 B. Prasad, R. M. Thakur, B. Mandal and B. Su, Enhanced CO2 separation membrane prepared from waste by-product of silk fibroin, *J. Membr. Sci.*, 2019, **587**, 117170, DOI: 10.1016/j.memsci.2019.117170.

67 H. Ohno and K. Fukumoto, Amino Acid Ionic Liquids, *Acc. Chem. Res.*, 2007, **40**, 1122–1129, DOI: 10.1021/ar700053z.

68 Y. S. Sistla and A. Khanna, CO2 absorption studies in amino acid-anion based ionic liquids, *Chem. Eng. J.*, 2015, **273**, 268–276, DOI: 10.1016/j.cej.2014.09.043.

69 M. S. Raja Shahrom, C. D. Wilfred, D. R. MacFarlane, R. Vijayraghavan and F. K. Chong, Amino acid based poly(ionic liquid) materials for CO2 capture: Effect of anion, *J. Mol. Liq.*, 2019, **276**, 644–652, DOI: 10.1016/j.molliq.2018.12.044.

70 Z. Tong and W. S. W. Ho, Facilitated transport membranes for CO2 separation and capture, *Sep. Sci. Technol.*, 2017, **52**, 156–167, DOI: 10.1080/01496395.2016.1217885.

71 S. Rafiq, L. Deng and M.-B. Hägg, Role of Facilitated Transport Membranes and Composite Membranes for Efficient CO2 Capture – A Review, *ChemBioEng Rev.*, 2016, **3**, 68–85, DOI: 10.1002/cben.201500013.

72 R. B. Said, J. M. Kolle, K. Essalah, B. Tangour and A. Sayari, A Unified Approach to CO_2–Amine Reaction Mechanisms, *ACS Omega*, 2020, **5**, 26125–26133, DOI: **10.1021/acsomega.0c03727**.

73 Y. Han and W. S. W. Ho, Polymeric membranes for CO_2 separation and capture, *J. Membr. Sci.*, 2021, **628**, 119244, DOI: **10.1016/j.memsci.2021.119244**.

74 H. M. Lee, I. S. Youn, M. Saleh, J. W. Lee and K. S. Kim, Interactions of CO_2 with various functional molecules, *Phys. Chem. Chem. Phys.*, 2015, **17**, 10925–10933, DOI: **10.1039/C5CP00673B**.

75 V. I. Bondar, B. D. Freeman and I. Pinnau, Gas transport properties of poly(ether-b-amide) segmented block copolymers, *J. Polym. Sci., Part B: Polym. Phys.*, 2000, **38**, 2051–2062, DOI: **10.1002/1099-0488(20000801)38:15<2051::AID-POLB100>3.0.CO;2-D**.

76 V. Barbi, S. S. Funari, R. Gehrke, N. Scharnagl and N. Stribeck, SAXS and the Gas Transport in Polyether-block-polyamide Copolymer Membranes, *Macromolecules*, 2003, **36**, 749–758, DOI: **10.1021/ma0213403**.

77 L. M. Robeson, The upper bound revisited, *J. Membr. Sci.*, 2008, **320**, 390–400, DOI: **10.1016/j.memsci.2008.04.030**.

78 Y. Chen, L. Zhao, B. Wang, P. Dutta and W. S. Winston Ho, Amine-containing polymer/zeolite Y composite membranes for CO_2/N_2 separation, *J. Membr. Sci.*, 2016, **497**, 21–28, DOI: **10.1016/j.memsci.2015.09.036**.

79 R. Nasir, H. Mukhtar and Z. Man, Fabrication, Characterization and Performance Study of N-methyl-diethanolamine (MDEA)-Polyethersulfone (PES) Amine Polymeric Membrane for CO_2/CH_4 Separation, *J. Appl. Sci.*, 2014, **14**, 1186–1191, DOI: **10.3923/jas.2014.1186.1191**.

80 G. Chen, T. Wang, G. Zhang, G. Liu and W. Jin, Membrane materials targeting carbon capture and utilization, *Adv. Membr.*, 2022, **2**, 100025, DOI: **10.1016/j.advmem.2022.100025**.

81 J. Shen, G. Liu, K. Huang, Q. Li, K. Guan, Y. Li and W. Jin, UiO-66-polyether block amide mixed matrix membranes for CO_2 separation, *J. Membr. Sci.*, 2016, **513**, 155–165, DOI: **10.1016/j.memsci.2016.04.045**.

82 J. Liu, X. Hou, H. B. Park and H. Lin, High-Performance Polymers for Membrane CO_2/N_2 Separation, *Chem.–Eur. J.*, 2016, **22**, 15980–15990, DOI: **10.1002/chem.201603002**.

83 S. L. Liu, L. Shao, M. L. Chua, C. H. Lau, H. Wang and S. Quan, Recent progress in the design of advanced PEO-containing membranes for CO_2 removal, *Prog. Polym. Sci.*, 2013, **38**, 1089–1120, DOI: **10.1016/j.progpolymsci.2013.02.002**.

84 H. A. Daynes and S. W. J. Smith, The process of diffusion through a rubber membrane, *Proc. R. Soc. London, Ser. A*, 1920, **97**, 286–307, DOI: **10.1098/rspa.1920.0034**.